

# Design of a segmented switched reluctance drive for a light electric vehicle

Pere Andrada

GAECE, Department of Electrical Engineering  
 EPSEVG, UPC BARCELONATECH  
 Avinguda Víctor Balaguer 1, Vilanova i la Geltrú 08800 (Spain)  
 Phone/Fax number: +0034 938967732, e-mail: [pere.andrada@upc.edu](mailto:pere.andrada@upc.edu)

**Abstract.** The light electric vehicle market requires better performance motors with less or even without permanent magnets. Switched reluctance motors (SRM) are among the best placed to meet this goal, despite they have lower power density, higher torque ripple, and are noisier than synchronous permanent magnet motors. Segmented stator switched reluctance motors (SSSRM) can reduce these drawbacks of conventional SRMs due to their modular construction and shorter flux paths. This paper presents a procedure for designing an SSSRM for a light electric vehicle. First, the output torque equation is derived from a simplified non-linear energy conversion loop, and then guidelines for its design are given. Once the preliminary sizing of the SSSRM has been carried out, simulation using electromagnetic finite element analysis is performed. Then, the complete drive is simulated and validated using Matlab-Simulink and some results of the definitive finite element analysis (magnetization curves and static torque curves).

**Key words.** Light electric vehicles, switched reluctance machines, segmented stator, design, finite element analysis.

## 1. Introduction

Global light-duty electric vehicle sales reached a record high of 6.3 million units in 2021; this number is expected to rise to 26.8 million units in 2030, according to the latest analysis from S&P Global Platts Analytics [1]. To achieve this goal is necessary to develop new low-cost, more efficient, and reliable drives with high torque to weight ratio. Nowadays, electric vehicle manufacturers are researching reducing and even suppressing the presence of permanent magnets in traction motors. The Switched Reluctance Motor (SRM) is well-positioned among the motors without permanent magnets despite its lower power density, high torque ripple, and acoustic noise [2, 3]. This paper deals with a particular type of switched reluctance motor with a segmented stator. The segmented stator switched reluctance motor (SSSRM) derives from the seminal work of Hendershot [4], to which later other authors made interesting contributions [5, 7]. The SSSRM comprises a stator with some independent and magnetically isolated cores (with C or U shape) and a rotor with salient poles. Coils are disposed of in the legs of the stator cores. They form, connected correctly, the phases of the machine. The right number of stator and rotor poles depends on the

number of phases and of the multiplicity. Fig. 1 shows the cross-section of a 12 stator and 10 rotor poles SSSRM. The advantages of SSSRMs compared to conventional SRMs are modular stator construction, short flux paths without flux reversal in the stator, and therefore fewer iron losses. To illustrate this, Fig. 1 depicts the distribution of magnetic field lines in a 12/10 SSSRM and Fig.2 in a conventional 12/8 SRM, in both cases when stator and rotor poles are in the aligned position. The construction of an SSSRM is not much more complicated than that of a conventional SRM, but the particular disposition of the stator limits the space for the windings. This paper proposes a new procedure, considering saturation, for sizing an SSSRM. The paper is organized in the following way: after this introduction, the design guidelines for the sizing of the SSSRM are given in Section 2. In Section 3, these guidelines are applied to a case study of the propulsion of a light electric vehicle. In Section 4, a simulation and validation of the drive are performed. Finally, in Section 5, the conclusions derived from this research are exposed.

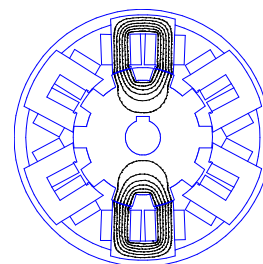


Fig. 1. Cross-section of a 12/10 SSSRM showing the distribution of the magnetic field lines.

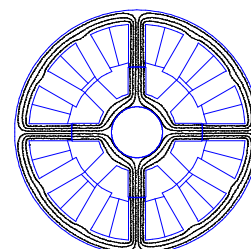


Fig. 2. Distribution of the magnetic field lines in a 12/8 SRM

## 2. Design procedure for SSSRM

As usual in electric machines, the proposed design procedure starts with determining the main dimensions using the output torque equation. Then simple geometrical relationships, proper of this kind of machine, and empirical knowledge allow the development of a first draft of the machine's geometry and its winding.

### A. Output torque equation

The starting point of the design of electric rotating machines is the output torque equation, which relates the torque with the main dimensions (inner stator diameter and axial length), magnetic loading, and electric loading. In this paper, following the procedure described in [8] for linear SRM and in [9] for axial flux SRM, the output torque equation of the SSSRM is obtained. Not of the average torque expression disregarding the saturation [10] but of the energy converted into mechanical work in each stroke, energy conversion loop, represented by the area  $W$  (OACEO) shown in Fig. 3, multiplied by the number of strokes,  $s$ , per revolution [11], that is:

$$T = s \cdot W \quad (1)$$

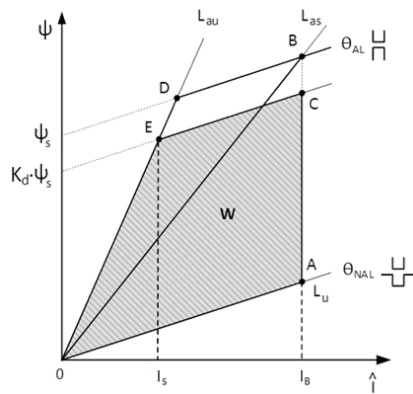


Fig. 3. Energy conversion loop

Neglecting phase resistance and considering two straight lines can approximate the aligned magnetization curve. OD with a slope  $L_{au}$ , and DB parallel to the unaligned magnetization curve, also a straight line, OA, with a slope  $L_u$ . From Fig. 3 can be deduced that the electromagnetic torque,  $T$ , in the SSSRM is given by:

$$T = \frac{\pi}{4} k_d k_L B_p A D^2 L \quad (2)$$

Where:

$k_d$  is the magnetic duty cycle

$k_L$  is a dimensionless coefficient that accounts for saturation:

$$k_L = \left(1 - \frac{L_u}{L_{au}}\right) \left(1 - \frac{1}{2} k_d \frac{L_{as} - L_u}{L_{au} - L_u}\right) \quad (3)$$

$B_p$ , Magnetic loading, magnetic flux density in a U-core leg.

$D$ , Inner diameter of the stator

$L$ , axial length

$A$ , electric loading:

$$A = \frac{2mN_f I_B}{\pi D} \quad (4)$$

With:

$m$ , Number of phases

$N_f$ , Number of turns per phase

$I_B$ , Current (see Fig.3)

The torque can be also expressed as:

$$T = C \cdot \frac{\pi}{4} D^2 L \quad (5)$$

With  $C$  torque per volume coefficient, equal to:

$$C = k_d k_L B_p A \quad (6)$$

Then the inner stator diameter of the stator can be determined by:

$$D = \sqrt[3]{\frac{4 \cdot T}{\pi \cdot \lambda \cdot C}} \quad (7)$$

With:

$$\lambda = \frac{L}{D} \quad (8)$$

### B. Design guidelines for sizing SSSRM

An  $m$ -phase SSSRM is formed by  $N_U$  independent U-shaped cores in the stator and  $N_R$  poles in the rotor with the angles that are shown in Fig. 4.

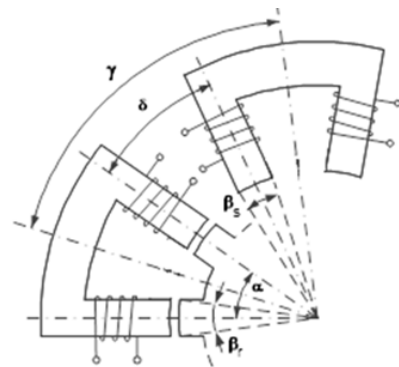


Fig. 4. Basic arrangement of an SSSRM.

In an  $m$ -phase SSSRM the following relationships must be fulfilled:

$$N_U = k \cdot m \quad (9)$$

With,  $N_U$  number of stator U-shaped stator cores and  $k$  multiplicity (number of working stator pole pairs).

The number of stator poles,  $N_s$ , is given by:

$$N_S = 2 \cdot k \cdot m \quad (10)$$

And the number rotor poles,  $N_R$ , is:

$$N_R = k \cdot (2m - 1) \quad (11)$$

The angle between axes of consecutive U-shaped cores,  $\gamma$ , is equal to:

$$\gamma = \frac{360^\circ}{N_U} \quad (12)$$

The angle between rotor poles,  $\alpha$ , is:

$$\alpha = \frac{360^\circ}{N_R} \quad (13)$$

And the angle between axes of stator poles of the two consecutive U-shaped cores,  $\delta$ , is given by:

$$\delta = \gamma - \alpha = \frac{360^\circ \cdot (N_R - N_U)}{N_U \cdot N_R} \quad (14)$$

A key point in the design of SRM machines are the stator,  $\beta_s$ , and rotor,  $\beta_r$ , pole angles. The stator pole angle,  $\beta_s$ , to get high window area to place the winding, should verify:

$$\beta_s < \frac{\alpha}{2} \quad (15)$$

The rotor pole angle,  $\beta_r$ , is recommended to be slightly larger than the stator pole angle, in order to guarantee the starting, that is:

$$\beta_r > \beta_s \quad (16)$$

Defining,  $k_\beta$ , the rotor to stator pole angle ratio, as:

$$k_\beta = \frac{\beta_r}{\beta_s} \quad (17)$$

In order to assure a high aligned to unaligned inductance relationship and self-starting capability [12],  $k_\beta$ , should be comprised between:

$$1 < k_\beta < 1.2 \quad (18)$$

The airgap,  $g$ , can be estimated with the same empirical formula used for three-phase asynchronous motors:

$$g(mm) = 0.2 + 2\sqrt{D(m) \cdot L(m)} \quad (19)$$

The stator width of the stator leg of a U-core,  $w_s$ , can be obtained by:

$$w_s = D \cdot \sin \frac{\beta_s}{2} \quad (20)$$

The stator back iron of a U-core,  $h_s$ , can be evaluated by:

$$h_s = (1 \div 1.25) \cdot w_s \quad (21)$$

The relationship between the inner stator diameter  $D$  and the output stator diameter,  $D_o$ , can be estimated for a 12/10 SSSRM as:

$$\frac{D}{D_o} = 0.56 \quad (22)$$

The length of a leg of a stator U-core,  $h_{ls}$ , is determined by:

$$h_{ls} = \frac{1}{2} (D_o - 2 \cdot h_s - D) \quad (23)$$

The rotor pole width,  $w_r$ , is obtained by:

$$w_r = (D - 2\delta) \cdot \sin \frac{\beta_r}{2} \quad (24)$$

And the rotor pole depth,  $h_{lr}$ , is estimated by:

$$h_{lr} = (1 \div 1.25) \cdot \frac{w_r}{2} \quad (25)$$

The voltage equation of the SSSRM can be approximated, being  $\omega$  the speed of the machine and neglecting phase resistance, by:

$$U = \frac{d\psi_s}{dt} + R_f I \approx \frac{\Delta\psi_s}{\Delta t} \approx \frac{\Delta\psi_s}{\Delta\theta} \quad (26)$$

From Figure 3, the increment of flux linkage between points A and C can be given by:

$$\Delta\psi_s = k_d L_{as} I_B = k_d N_f B_p D L \frac{\beta_s}{2} \quad (27)$$

And the variation of position between points A and C by:

$$\Delta\theta \approx k_d \beta_s \quad (28)$$

Then the number of turns per phase,  $N_f$ , is given by:

$$N_f = \frac{2U}{B_p D L \omega} \quad (29)$$

And the number of turns per coil is:

$$N_p = \frac{m N_f}{2 N_U} \quad (30)$$

Large number of turns provides high torque at low speeds but low speed range at constant power.

The section of the conductors is selected fixing a current density ( $A/mm^2$ ) according to the cooling conditions of the machine.

### 3. Case study

The explained procedure is applied to the case of a SSSRM for the propulsion of a light electric vehicle. The requirements of the motor are maximum torque of 27.9 Nm between 0 and 1396 rpm and constant power of 4 kW between 1396 rpm and 4063 rpm. The motor has to be powered by a Li-ion battery pack of 72 V. The motor is naturally air-cooled. The power converter is an asymmetric half bridge. The control is by hysteresis with variable turn-on and turn-off angles at low and medium speeds and single pulse control with also variable turn-on and turn-off angles at high speeds [13].

In this case a three-phase SSSRM with multiplicity 2 is considered, 12/10 SSSRM. For this application, it is also advisable that  $D > L$ , then  $\lambda$  is taken equal  $\frac{1}{2}$ . Electric steel non-oriented fully processed M250-50 A is selected for the construction of the stator U-cores and the rotor pack because of low iron losses and its reasonable cost.

The first step is to determine the main dimensions, the inner diameter of the stator,  $D$ , and the axial length,  $L$ , for which the point of maximum torque at maximum speed (1396 rpm, 27.9 Nm) is considered. For that, the following assumptions should be made:

$$\begin{aligned}
 B_p &= 1.7 \text{ T (slightly lower than saturation flux density of M250-50)} \\
 A &= 67 \text{ kA/m (naturally air-cooled)} \\
 k_d &= 0.9 \\
 k_L &= 0.4 \\
 \lambda &= 1/2
 \end{aligned}$$

With these values and from equations (5), (6) and (7) the inner stator diameter and the axial length are obtained:

$$D = 120 \text{ mm; } L = 60 \text{ mm}$$

In Table I are listed the values of  $N_s$ ,  $N_r$ ,  $\alpha$ ,  $\gamma$ ,  $\delta$ ,  $\beta_s$  and  $\beta_r$  corresponding to a three-phase 12/10 SSSRM with multiplicity 2 calculated according to equations (13-19).

Table I.- Values of  $N_s$ ,  $N_r$ ,  $\alpha$ ,  $\gamma$ ,  $\delta$ ,  $\beta_s$ ,  $\beta_r$

|                | $N_s$ | $N_r$ | $\alpha$ | $\gamma$ | $\delta$ | $\beta_s$ | $\beta_r$ |
|----------------|-------|-------|----------|----------|----------|-----------|-----------|
| $m=3$<br>$k=2$ | 12    | 10    | 36°      | 60°      | 24°      | 15°       | 16°       |

The airgap,  $g$ , estimated according to (19), is equal to 0.37 mm, but for this application, it is better to consider a little bigger value, for instance, 0.5 mm

In Table II are compiled the values of  $w_s$ ,  $h_s$ ,  $h_{ls}$ ,  $w_r$  and  $h_{lr}$  calculated by means of expressions (20-25).

Table II.- Values of  $w_s$ ,  $h_s$ ,  $h_{ls}$ ,  $w_r$ ,  $h_{lr}$

|               |       |
|---------------|-------|
| $w_s$ (mm)    | 15.66 |
| $h_s$ (mm)    | 17.62 |
| $h_{ls}$ (mm) | 29.38 |
| $w_r$ (mm)    | 16.56 |
| $h_{lr}$ (mm) | 9.31  |

The number of turns per coil calculated utilizing the expressions (29) and (30) is equal to 8, considering that the SSSRM is developing 4 kW at 4063 rpm, and the estimated magnetic flux density in these conditions is 1.5 T.

The section of the conductors is selected, fixing a current density (RMS value) of  $6A/mm^2$ , resulting in a wire section of  $10 \text{ mm}^2$ .

#### 4. Simulation and validation of the SSSRM

Once defined a preliminary geometry and the winding arrangement of the SSSRM, the whole drive, including the motor, the power converter, and taking into account the control strategies, is simulated. This simulation is first an electromagnetic finite element analysis [14], allowing refining or modifying some geometrical parts of the machine and introducing some constructional solutions as holes for fixation of the U-shaped cores and the rotor pack and voids to lighten up and ease cooling of the rotor. Fig. 5 shows the distribution of the magnetic field lines for a position  $9^\circ$  from unalignment and a current of 100 A. Then, the complete drive is simulated using Matlab-Simulink and some results of the definitive finite element analysis (magnetization curves, Fig. 6, and static torque curves, Fig. 7). These simulations evaluate the drive's behaviour in different operating conditions and define the best values for the turn-on and turn-off angles. They can also help decide the final numbers of turns per pole to better adjust to the requirements of the drive, being in our case 10 compared to the 8 initially calculated. In Fig. 8, the phase voltage, torque, phase current, flux, and dc bus current corresponding to the point of the maximum speed at which the maximum torque can be maintained (1400 rpm, 28 Nm) are shown. These values are achieved using hysteresis control, a reference current of 175 A, and turn-on and turn-off angles of  $-2^\circ$  and  $15^\circ$ , respectively (the  $0^\circ$  corresponds to the unaligned position).

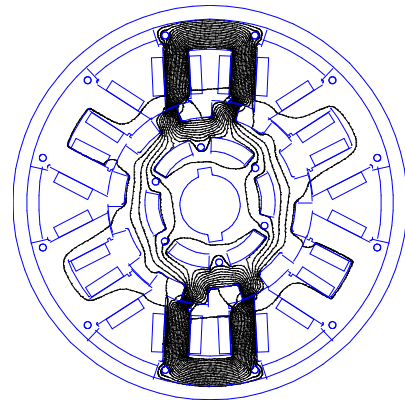


Fig. 5. Distribution of magnetic flux field lines for a position  $9^\circ$  from unalignment in the SSSRM.

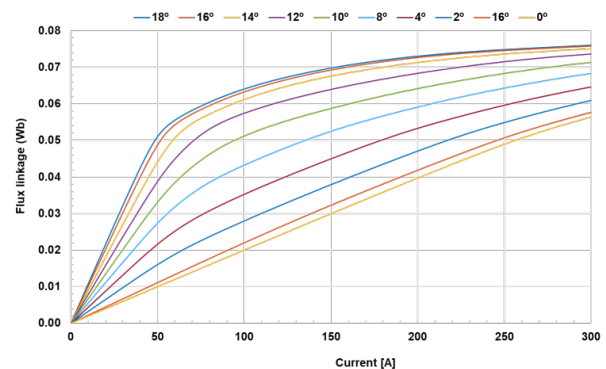


Fig. 6. Magnetization curves of the final SSSRM design.

In table III, the final values of the design of the SSSRM drive are collected observing slight changes with respect to the values initially determined following the proposed guidelines.

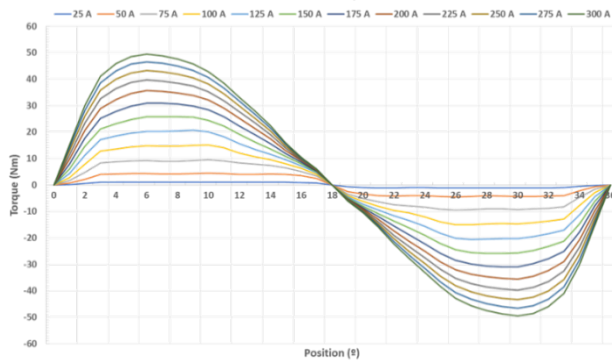


Fig.7. Static torque curves of the final SSSRM design

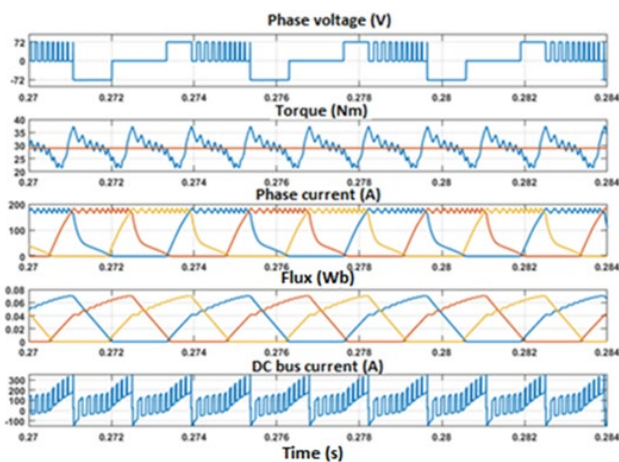


Fig. 8. Simulated values of phase voltage, torque, phase current, flux and dc bus current for a torque of 28 Nm at 1400 rpm.

Table III.-Main data of the designed 12/10 SSSRM

| Parameter  | Values                                     |
|--|--|
| U, Rated voltage (V)                                 | 72   |
| m, Number of phases                                  | 3  |
| $N_{U_i}$ , Number of stator U shaped cores          | 6  |
| $N_s$ , Number of stator poles                       | 12   |
| $N_R$ , Number of rotor poles                        | 10   |
| $\alpha(^{\circ})$                                   | 36   |
| $\gamma(^{\circ})$                                   | 60   |
| $\delta(^{\circ})$                                   | 24   |
| $D_i$ , Inner stator diameter (mm)                   | 120  |
| L, stator axial length (mm)                          | 60   |
| $D_r$ , Rotor diameter (mm)                          | 119  |
| $D_o$ , Output stator diameter (mm)                  | 214  |
| g, Airgap (mm)                                       | 0.5  |
| $\beta_s$ , Stator polar angle ( $^{\circ}$ )        | 15   |
| $\beta_R$ , Rotor polar angle ( $^{\circ}$ )         | 16   |
| $w_s$ , stator polar width(mm)                       | 15.11                                      |
| $w_R$ , Rotor pole width (mm)                        | 16.56                                      |
| $h_s$ , Stator back iron of a U-core (mm)            | 17.5                                       |
| $h_{ls}$ , Length of the leg of a stator U-core (mm) | 29.5                                       |
| $h_{lr}$ , Rotor pole depth (mm)                     | 9.5  |
| $D_s$ , Shaft diameter (mm)                          | 35   |
| $N_p$ , Number of turns per pole                     | 10   |
| $n_p$ , Number of coils per phase                    | 4  |
| $N_f$ , Number of turns per phase                    | 40   |
| $S_c$ , Wire section (mm)                            | 2 wires, each one 2x2.4 (rectangular wire) |
| Thermal class of isolation                           | 180 $^{\circ}$ C                           |

## 5. Conclusion

This paper presents a procedure for designing an SSSRM. This procedure starts with determining the main dimensions using the output torque equation derived from a simplified non-linear energy conversion loop. The next step consists of obtaining simple geometrical relationships proper for this kind of machine that, along with empirical knowledge, allow the development of a first draft of the machine's geometry and its winding. Then, the complete drive is simulated using Matlab-Simulink and some results of the definitive finite element analysis, magnetization curves and static torque curves. The design procedure has been applied to the case of an SSSRM drive for the propulsion of a light electric vehicle. Simulations show that the performance of the designed SSSRM matches pretty well with the expected requirements.

## Acknowledgement

The author wishes to thank Professor Marcel Torrent for allowing the use of the 12/8 SRM simulation (Fig. 2) and student Pol Kobeaga for performing the simulations with the 12/10 SSSRM (Figures 5 to 8).

## References

- [1] S&P Global Commodity Insights, February 16, 2022.
- [2] P. Andrada, M.J. Dougan, F.J. Márquez-Fernández, A. Egea, L.Szabó. "Are SRM drives a real alternative for EV powertrain?" Workshop on SRM drives an alternative for E-traction. Vilanova i la Geltrú, Spain. February 2, 2018.
- [3] P. Andrada. "Trends in Switched Reluctance Motor Drives for Electric Traction". Chapter 1, SRM drives for electric traction. Edited P.Andrada, Iniciativa Digital Politècnica 2019.
- [4] J.R. Hendershot. "Short flux paths cool SR motors". Machine Design. September 1989. pp.106-111.
- [5] T. Burrell and C. Ayers. "Development and experimental characterization of a multiple isolated flux path reluctance machine". 2012 IEEE Energy Conversion Congress and Exposition, pp. 899-905.
- [6] M. Ruba, I. A. Viorel, L. Szabó. "Modular stator switched reluctance motor for fault tolerant drive Systems". IET Electric Power Applications, 2013, Vol. 7, Iss. 3, pp. 159-169.
- [7] R. Jæger, S.S. Nielsen, P. O. Rasmussen, K. Kongerslev. "Development and analysis of U-core switched reluctance machine". 2016 IEEE Energy Conversion Congress and Exposition (ECCE).
- [8] J. Garcia Amorós, P. Andrada, B. Blanqué. "Design procedure for a longitudinal flux flat linear switched reluctance motor". Electric Power Components and Systems, 40, 2012, 161-178.
- [9] P. Andrada, B. Blanqué, E. Martínez, J.I. Perat, J. A. Sánchez and M. Torrent. "Design of a Novel Modular Axial-Flux Double Rotor Switched Reluctance Drive". Energies 2020, 13, 1161.
- [10] R. Krishnan, R. Arumugan, J.M. Lindsay. "Design procedure for switched-reluctance motors". IEEE Transactions on Industry Applications, 24, 3, 1988, May/June, 456-461.
- [11] T.J.E. Miller. "Converter volt-ampere requirements of the switched reluctance motor drive". IEEE Transactions on

Industry Applications, 21, 5, 1985, September/October, 1136-1144.

- [12] X.D. Xue, W.E. Cheng and N.C. Cheung. "Multi-objective optimization design of in-wheel switched reluctance motors in electric vehicles". IEEE Transactions on Industrial Electronics, vol 57, no 9, pp 2980-2987, Sep.2010.
- [13] P. Andrada, B. Blanqué, M. Capó, G. Gross, D. Montesinos. "Switched Reluctance Motor Controller for Light Electric Vehicles." 2018 20th European Conference on Power Electronics and Applications (EPE'18 ECCE Europe), 2018. pp.1-11.
- [14] FEMM (Finite Element Method Magnetics) home page. <http://www.femm.info/wiki/HomePage>.